Journal of Dental Sciences 21 (2026) 305–314

Available online at www.sciencedirect.com

ScienceDirect

journal homepage: www.e-jds.com

Original Article

Novel *MMP20* (matrix metalloproteinase 20) mutations causing hypoplastic-hypomaturation amelogenesis imperfecta

Shih-Kai Wang [a,b*], Hong Zhang [c], Hua-Chieh Lin [a], Yin-Lin Wang [a,b], J. Timothy Wright [d], John D. Bartlett [e], James P. Simmer [c], Jan C.-C. Hu [c]

[a] *Department of Dentistry, National Taiwan University School of Dentistry, Taipei City, Taiwan*
[b] *Department of Pediatric Dentistry, National Taiwan University Children's Hospital, Taipei City, Taiwan*
[c] *Department of Biologic and Materials Sciences, University of Michigan School of Dentistry, Ann Arbor, MI, USA*
[d] *Department of Pediatric Dentistry, University of North Carolina School of Dentistry, Chapel Hill, NC, USA*
[e] *Division of Biosciences, The Ohio State University, College of Dentistry, Columbus, OH, USA*

Received 9 August 2025; Final revision received 24 August 2025
Available online 11 September 2025

KEYWORDS
Metzincin;
Enamel matrix proteins;
Biomineralization;
Pathogenic variant;
Catalytic domain;
Proteolysis

Abstract *Background/purpose:* Matrix metalloproteinase 20 (MMP20) is a proteinase essential for dental enamel formation. Mutations in human *MMP20* cause autosomal recessive amelogenesis imperfecta (AI), characterized by thin and soft enamel. This study aimed to unravel the genetic causes for five families with hypoplastic-hypomaturation AI.
Materials and methods: Whole-exome analyses and Sanger sequencing were performed to identify and confirm disease-causing mutations. To evaluate the pathogenicity of identified *MMP20* missense variants, immunoblotting and gelatin zymography were conducted on proteins overexpressed in HEK293T cells.
Results: All affected individuals from the five families exhibited similar dental phenotypes, including chalky-white to yellow-brown discolorations and evident dental attrition. The defective enamel was both thin and hypomineralized. Six pathogenic *MMP20* variants were identified: c.289A>T (p.Lys97*), c.547G>A (p.Asp183Asn), c.686G>A (p.Gly229Asp), c.102G>A (p.Trp34*), c.359dup (p.Asn120Lysfs*9), and c.954-2A>T. Among them, the first three have not been previously reported. The two missense mutations altered evolutionarily conserved amino acid residues within the catalytic domain of MMP20. Compared with the wild type,

* Corresponding author. Department of Dentistry, National Taiwan University School of Dentistry, No.1, Changde St., Jhongjheng District, Taipei City 100229, Taiwan.
E-mail address: shihkaiw@ntu.edu.tw (S.-K. Wang).

https://doi.org/10.1016/j.jds.2025.08.039

secretion of both mutant MMP20 proteins was significantly impeded, and neither displayed proteolytic activity on gelatin zymography, indicating a loss of enzymatic function.
Conclusion: This study expands the genotypic spectrum of *MMP20*-associated AI and highlights two critical residues within the MMP20 catalytic domain that are essential for its secretion and enzymatic activity.

Introduction

Dental enamel formation, known as amelogenesis, is a matrix-mediated biomineralization process.[1] During this process, enamel matrix proteins (EMPs), namely amelogenin, ameloblastin, and enamelin, are secreted, processed, degraded, and ultimately removed to facilitate the growth of hydroxyapatite crystals and allow enamel to achieve a high degree of mineralization.[2] MMP20 (matrix metalloproteinase 20) is the predominant proteinase responsible for processing EMPs during the secretory stage of amelogenesis.[3–5] *Mmp20* ablation in mice leads to severely hypoplastic and dysplastic enamel that contains uncleaved EMPs in developing teeth, further demonstrating its critical role in enamel formation.[6–8] Additionally, loss-of-function mutations in human *MMP20* (OMIM ∗604629) cause autosomal recessive amelogenesis imperfecta (AI) (OMIM #612529), resulting in various enamel malformations, including hypoplastic (thin), hypomaturation (soft), or combined hypoplastic-hypomaturation defects.[9,10] Recently, it was reported that patients with biallelic *MMP20* mutations and *Mmp20* null mice also exhibit dentin defects, suggesting its role in dentinogenesis.[11] However, *MMP20* is pseudogenized in species that have lost their teeth during

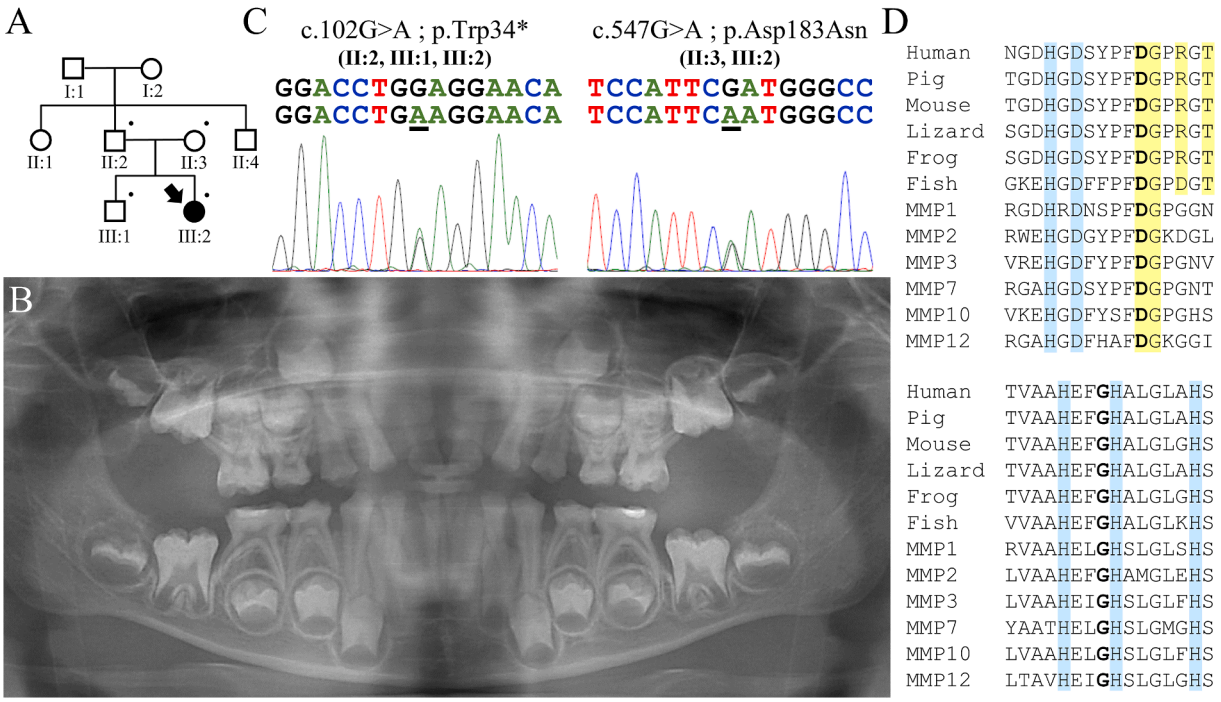

Figure 1 Family 1 with compound heterozygous *MMP20* p.Trp34* and p.Asp183Asn mutations. (**A**) The family pedigree shows that the proband (III:2; 5-year-old girl) was the only affected individual with enamel defects in family. (**B**) The proband's panoramic radiograph demonstrates that the enamel of both her primary and developing permanent teeth was abnormally thin and exhibited little radiographic contrast with the dentin, indicating hypoplastic-hypomaturation AI. (**C**) The DNA sequencing chromatograms exhibit two G-to-A transitions, c.102G>A and c.547G>A, which cause a p.Trp34* truncation and a p.Asp183Asn substitution in *MMP20* respectively. (**D**) Amino acid sequence alignment of MMP20 orthologs from human (NP_004762.2), pig (NP_999070.1), mouse (NP_038931.1), lizard (XP_028581561.1), frog (NP_001091444), and fish (XP_009290029.1) along with human MMP20 paralogs, including MMP1 (NP_002412.1), MMP2 (NP_004521.1), MMP3 (NP_002413.1), MMP7 (NP_002414.1), MMP10 (NP_002416.1), and MMP12 (NP_002417.2). The substituted amino acids in p.Asp183Asn (top), and p.Gly229Asp (bottom) are in bold. The residues that coordinate the zinc and calcium ions are highlighted in blue and yellow respectively.

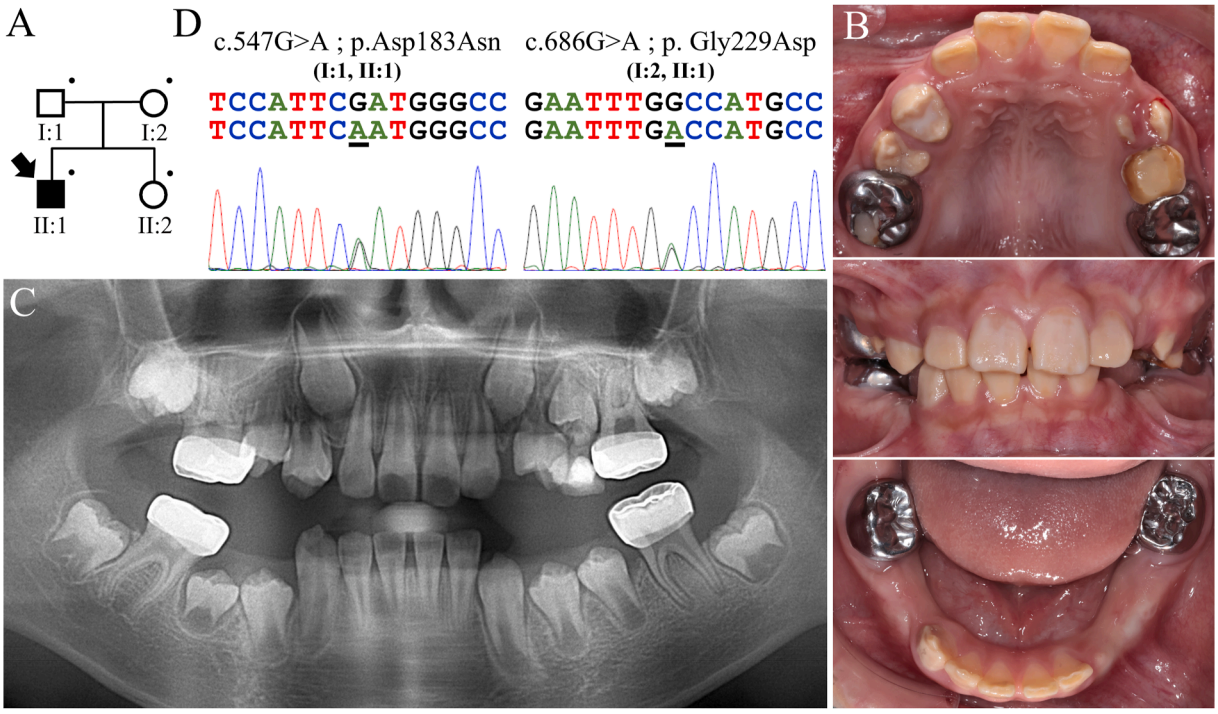

Figure 2 Family 2 with compound heterozygous *MMP20* p.Asp183Asn and p.Gly229Asp substitution mutations. (**A**) The family pedigree indicates a simplex case of enamel malformations. (**B**) Intraoral photographs of the proband (II:1; 10-year-old boy) demonstrate that his permanent teeth appeared opaque and yellowish, lacking the translucent shine of normal enamel. Dental attrition was evident at the incisal edges of both the maxillary and mandibular incisors. All first permanent molars have been restored with stainless steel crowns due to excessive wear. (**C**) The proband's panoramic radiograph reveals that all his teeth had thin, less radiopaque enamel, confirming the diagnosis of hypoplastic-hypomaturation AI. (**D**) The DNA sequencing chromatograms show two G-to-A transitions, c.547G>A and c.686G>A, which cause *MMP20* missense mutations, p.Asp183Asn and p.Gly229Asp, respectively.

evolution, indicating that it is essential only for tooth formation.[12,13]

Similar to other MMPs, the protein structure of MMP20 comprises a signal peptide, a propeptide, followed by the catalytic and hemopexin-like domains, which are linked by a hinge region.[14] The propeptide domain of MMP20 contains the conserved sequence PRCGVPDV, which is considered critical for maintaining enzyme latency, although its precise function remains unclear. In contrast, the catalytic domain is essential for MMP20's proteolytic function and is structurally conserved across all orthologs and paralogs.[15] This domain contains two zinc ions, two calcium ions, and the consensus motif HEFGHALGLAH at the active site. Multiple human *MMP20* mutations that substitute highly conserved amino acid residues within this domain have been shown to significantly reduce enzymatic activity and cause AI.[16,17] Like the propeptide domain, the function of the hemopexin-like domain at the C-terminus of MMP20 is less well understood. It has been demonstrated that this region is susceptible to autoproteolysis, and MMP20 lacking this domain can still precisely cleave EMPs, indicating its dispensable role in proteolysis.[18] However, the discovery of AI-causing mutations within this domain suggests that the hemopexin-like domain may play an essential role beyond proteolytic function during enamel formation.[11,19]

In this study, we identified and characterized five AI kindreds with hypoplastic-hypomaturation enamel defects caused by biallelic *MMP20* mutations. Molecular analyses of the missense mutations not only confirmed their pathogenicity but also revealed the functional importance of the affected amino acid residues within the MMP20 catalytic domain.

Materials and methods

Subject recruitment and mutational analyses

The research protocols and consent forms for human studies were reviewed and approved by the Institutional Review Boards at National Taiwan University Hospital (201605017RINC) and the University of Michigan (H03-00001835-M1). All study procedures adhered to the specified protocols and complied with the Declaration of Helsinki. Participants were provided with comprehensive explanations and discussions about the research contents, after which written consent was obtained from each. Clinical and radiographical examinations were conducted and family history reviewed for phenotyping and constructing kindred pedigrees. Each subject provided 2 mL of non-stimulated saliva for genomic DNA extraction to perform mutational analyses.

To identify AI-causing mutations, whole exome sequencing and analyses were conducted for each family as previously described.[11] The identified *MMP20* pathogenic variants were confirmed by Sanger sequencing and described using human reference sequences, NG_012151.1,

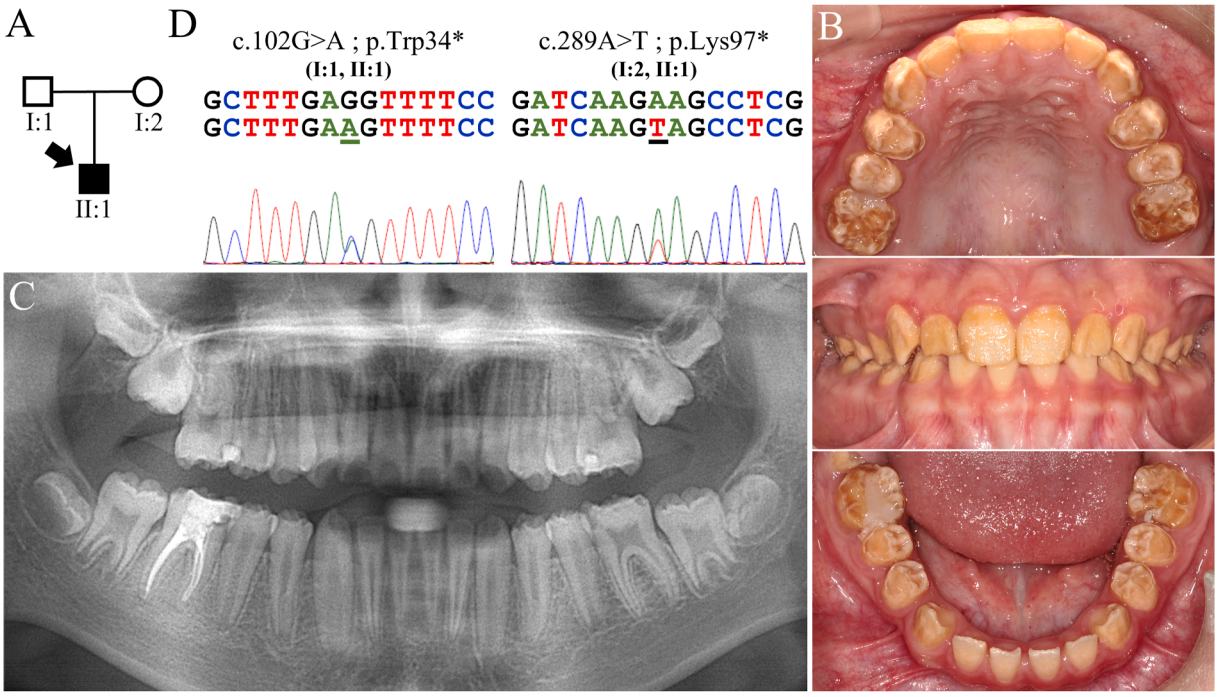

Figure 3 Family 3 with compound heterozygous *MMP20* p.Trp34* and p.Lys97* mutations. (**A**) The family pedigree shows a trio with the proband as the only affected individual among extended family members. (**B**) Intraoral photographs of the proband (II:1; 12-year-old boy) indicate yellowish-brown and opaque tooth discoloration with a rough surface texture. Severe dental attrition and enamel chipping are evident on all teeth, indicating a hypomineralized enamel defect. (**C**) The proband's panoramic radiograph reveals generalized thin enamel layers with reduced radiocontrast relative to the underlying dentin, confirming the diagnosis of hypoplastic-hypomaturation AI. (**D**) The DNA sequencing chromatograms show heterozygous *MMP20* c.102G>A and c.289A>T variants, which cause two nonsense mutations, p.Trp34* and p.Lys97*, respectively.

NM_004771.4, and NP_004762.2. The distribution of the mutations within the family was further analyzed.

Protein overexpression and Western blot analyses

A 1495-bp DNA fragment containing the human *MMP20* open reading frame (CCDS8318.1) was synthesized and cloned into the pcDNA3.1(+) vector using NheI and XhoI restriction sites, resulting in a construct expressing a C-terminally FLAG-tagged MMP20 protein. Site-directed mutagenesis was subsequently performed to introduce the c.547G>A and c.686G>A variants into the wild-type construct, generating two mutant clones encoding the p.Asp183Asn and p.Gly229Asp substitutions, respectively. HEK293T cells (CRL-3216; ATCC, Manassas, VA, USA) were used for protein overexpression. The cells were cultured in 6-well plates and transfected at 70 % confluence using Lipofectamine™ 3000 reagent (L3000015; Thermo Fisher Scientific, Waltham, MA, USA). After 24 h, the culture medium was replaced with CD 293 protein-free medium (11913019; Thermo Fisher Scientific).

Following another 48 h, the culture medium from each well was collected and concentrated from 4 mL to 25 μL using an Amicon® Ultra Centrifugal Filter (30 kDa) concentrator (UFC5030; Millipore, Burlington, MA, USA). The transfected cells were harvested and lysed using 50 μL of RIPA cell lysis buffer (RB4476; Bio Basic, Markham, Ontario, Canada) containing a protease inhibitor cocktail (C0001; TargetMol, Boston, MA, USA). The proteins from both the culture medium and cell lysates were quantified using the Bio-Rad protein assay kit (5000001; Bio-Rad, Hercules, CA, USA). For protein detection, 50 μg of total proteins from cell lysates and proteins from 5 μL of concentrated culture media were separated via SDS-PAGE electrophoresis and transblotted onto PVDF membranes, followed by standard immunoblotting procedures.

The primary antibodies used for immunoblotting include anti-DDDDK tag (1:1000; GTX115043; GeneTex, Irvine, CA, USA), anti-beta actin (1:5000; ab8226; Abcam, Cambridge, UK), and anti-MMP20 (1:1000; DF7694; Affinity Biosciences, Cincinnati, OH, USA) antibodies. HRP-conjugated goat anti-rabbit IgG (1:5000; SA00001-2; Proteintech, Rosemont, IL, USA) and HRP-conjugated goat anti-mouse IgG (1:5000; SA00001-1; Proteintech) were used as secondary antibodies.

Gelatin zymography

Following 72 h of transfection, the cells overexpressing MMP20s were harvested and lysed using RIPA buffer without protease inhibitors. To assess proteolytic activity, 3 μg of total protein from each cell lysate was loaded onto Novex™ 10 % Zymogram Plus (Gelatin) Protein Gels (ZY00100BOX; Thermo Fisher Scientific) and separated under denaturing conditions. After electrophoresis, the gel was renatured for 30 min and incubated in developing buffer overnight before stained using the Colloidal Blue Staining Kit (LC6025;

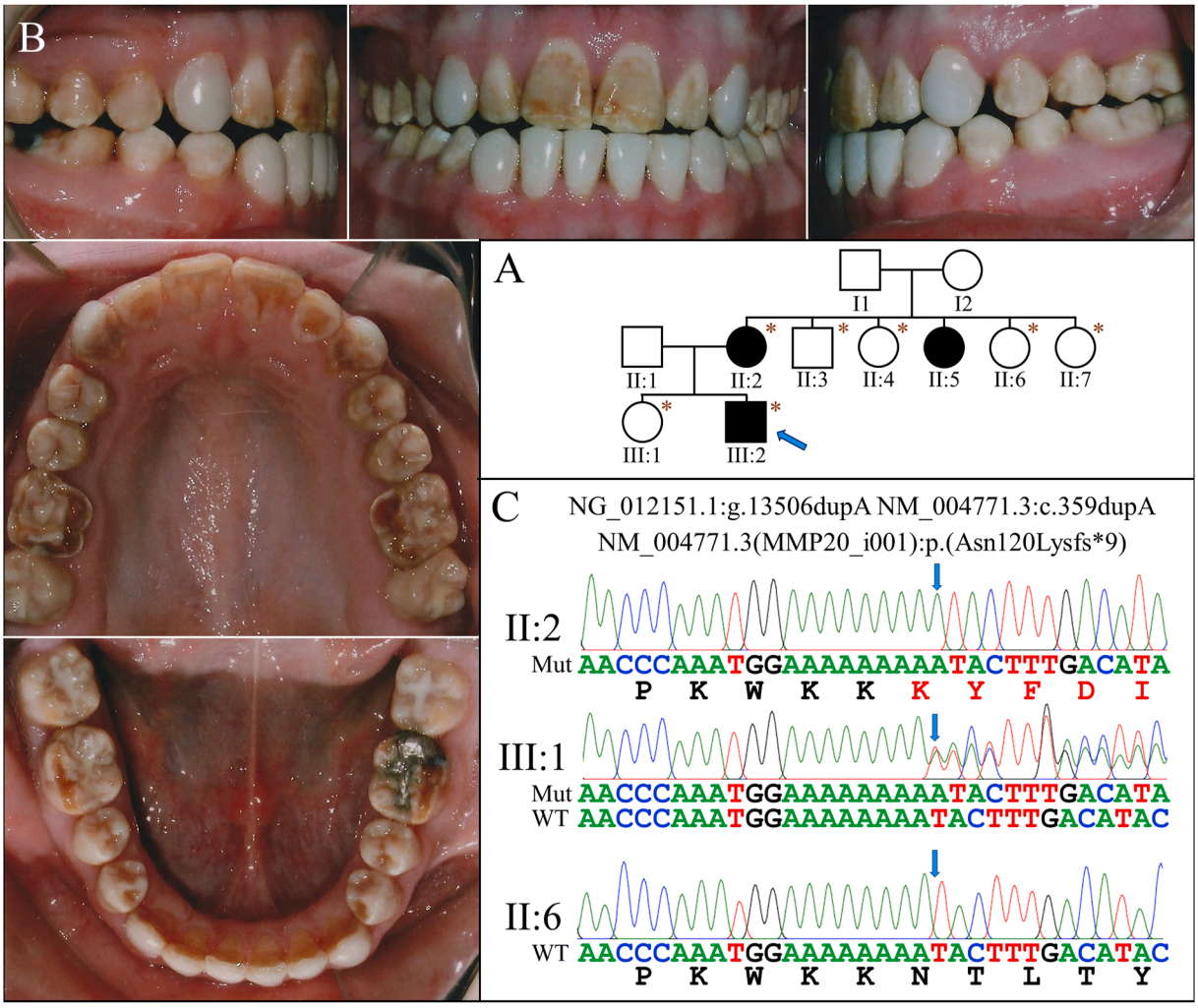

Figure 4 Family 4 with homozygous *MMP20* p.Asn120Lysfs*9 mutation. (**A**) The family pedigree (incorrectly) suggests a likely dominant pattern of disease inheritance from the maternal side, although the condition is recessive with the same *MMP20* frameshift mutation presumably contributed by both parents. Subjects I:1, I:2, and II:1, who are likely carriers, were unable to participate in this study. (**B**) Intraoral photographs of the proband (III:2) revealed white-yellowish tooth discoloration and thin enamel, consistent with hypoplastic-hypomaturation AI. The first molars exhibited severe dental attrition. The facial surfaces of maxillary canines and mandibular anterior teeth were restored with dental veneers to enhance esthetics. (**C**) The DNA sequencing chromatograms demonstrate a single nucleotide duplication (c.359dup) in Exon 2 of *MMP20* in homozygous (top), heterozygous (middle), and wild-type individuals (bottom). The mutation causes a frameshift and premature translation termination, p. Asn120Lysfs*9, which would likely render the mutant transcript to nonsense-mediated decay.

Thermo Fisher Scientific) for ~48 h until clear bands were visible. In parallel, identical amounts of protein samples were analyzed via SDS-PAGE electrophoresis on a 10 % Tris-base gel, followed by anti-MMP20 immunoblotting to quantify the overexpressed MMP20s in each cell lysate.

Results

Family 1

The proband of Family 1 was a 5-year-old girl who was the only individual with enamel malformations in her family (Fig. 1A). She was generally healthy, and the family history was not contributory. At the primary dentition stage, her deciduous teeth appeared to have thin enamel. Carious lesions could be found in most teeth, while dental attrition and sporadic enamel chipping were also evident. Radiographically, the enamel of the unerupted permanent teeth was abnormally thin and had reduced contrast with underlying dentin, indicating both hypoplastic and hypomaturation enamel defects (Fig. 1B).

Exome sequencing and analysis demonstrated that the proband was a compound heterozygote for two *MMP20* sequence variants at Exons 1 and 4 (Fig. 1C). The first one (NG_012151.1:g.5115G>A, NM_004771.4:c.102G>A) was a nonsense mutation that introduces a premature stop codon and truncates the protein (NP_004762.2:p.Trp34*), while the other (g.20326G>A, c.547G>A) a missense defect that changes codon 183 (p.Asp183Asn). Both mutations are rare

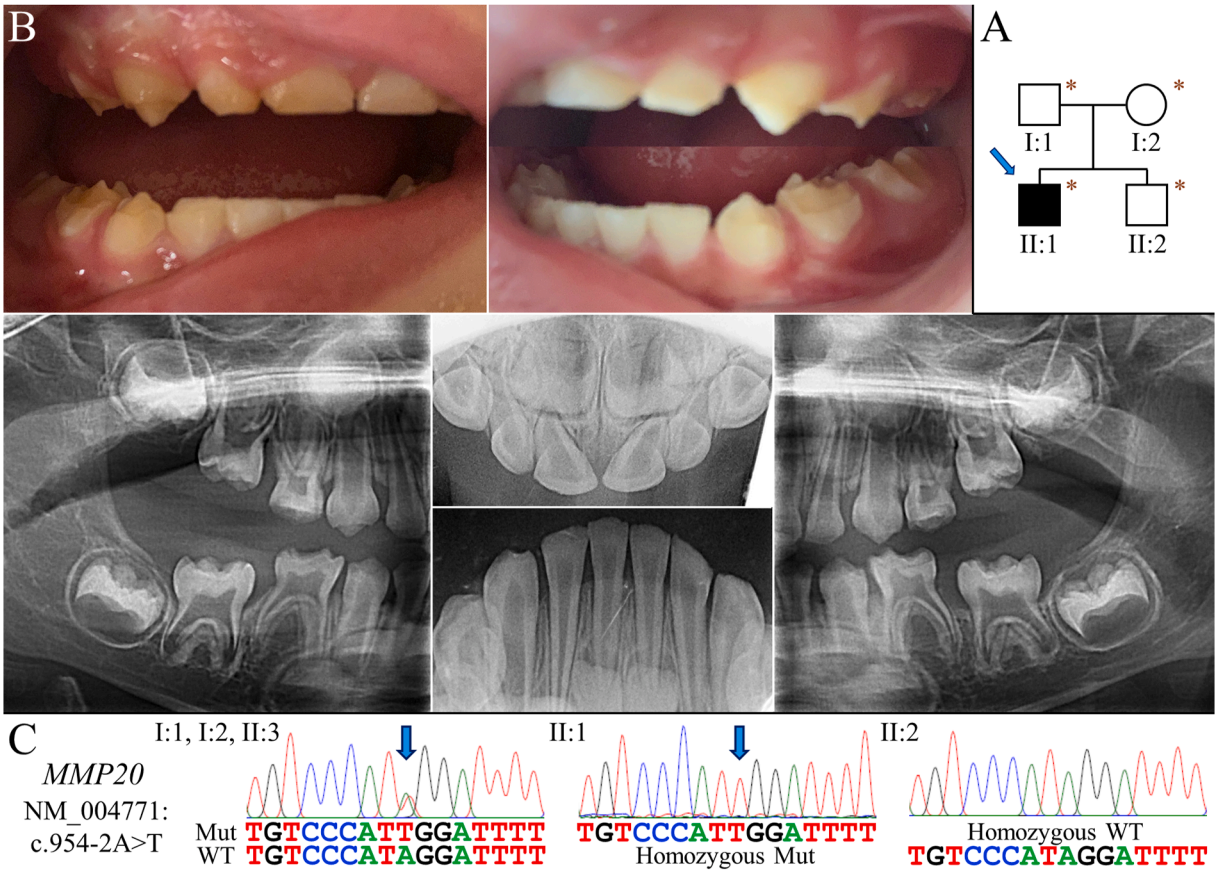

Figure 5 Family 5 with homozygous *MMP20* c.954-2A>T mutation. (**A**) The family pedigree displays a simplex case of enamel malformations, with no reported consanguinity. (**B**) Intraoral photographs of the proband (II:1) reveal severe dental attrition and enamel chipping on his primary teeth, indicating a hypomineralized defect. Both periapical and panoramic radiographs show abnormally thin enamel with reduced radiopacity across all teeth, including developing permanent teeth, confirming the clinical diagnosis of hypoplastic-hypomaturation AI. (**C**) The DNA sequencing chromatograms exhibit an A-to-T transversion (c.954-2A>T) at the splice acceptor site of *MMP20* Intron 6, shown in heterozygous (left), homozygous (middle), and wild-type (right) individuals. The mutation has been reported to cause AI in many cases of various ethnicities.

sequence variants documented in the gnomAD database with minor allele frequencies (MAFs) of 0.00045 (rs587777516) and 0.0002 (rs767412802) in EAS population respectively.[20] The p.Trp34∗ mutation was previous reported in a sporadic case with hypoplastic-hypomaturation AI who was homozygous for the *MMP20* defect.[21] The mutant transcript would most likely undergo nonsense mediated decay (NMD) and produce no protein. On the other hand, the p.Asp183Asn mutation replaces an aspartic acid residue that is highly conserved across both MMP20 orthologs and paralogs (Fig. 1D) and is predicted to be "likely pathogenic" by the AlphaMissense algorithm with an pathogenicity score of 0.9358.[22] Segregation analysis indicated that this missense variant was maternally inherited, while the father (II:2) and brother (III:1) were heterozygous for the nonsense mutation. Only the proband, who had enamel malformations, carried both defective *MMP20* alleles, demonstrating their pathogenicity.

Family 2

Family 2 was a nuclear family of which the proband (II:1), a 10-year-old boy, had enamel defects but was otherwise healthy (Fig. 2A). Clinically, all his primary teeth have shed except for Tooth J, which had almost no enamel coverage due to severe dental attrition and chipping. The permanent teeth appeared chalky white and yellowish, lacking the translucency from normal enamel (Fig. 2B). Despite recent emergence, the incisal edges of the incisors and occlusal surfaces of the first molars exhibited significant wear to the extent that the molars had to be protected with stainless steel crowns. Consistently, the panoramic radiograph showed that the enamel of the unerupted permanent teeth was not only less radiopaque but thinner than normal, confirming a diagnosis of hypoplastic-hypomaturation AI (Fig. 2C). None of the other three family members had similar dental phenotypes.

Analysis of proband's exome revealed two single nucleotide variants in *MMP20*, g.20326G>A (c.547G>A) and g.21271G>A (c.686G>A) (Fig. 2D). The first variant was identical to the missense mutation, p.Asp183Asn, found in Family 1. The other was an unreported mutation at Exon 5 that substitutes an aspartic acid for a glycine, p.Gly229Asp. This rare sequence variant (rs549925622) has a MAF of 0.000156 in EAS population of gnomAD. Similar to Asp^{183}, Gly^{229} is also highly conserved across vertebrate evolution

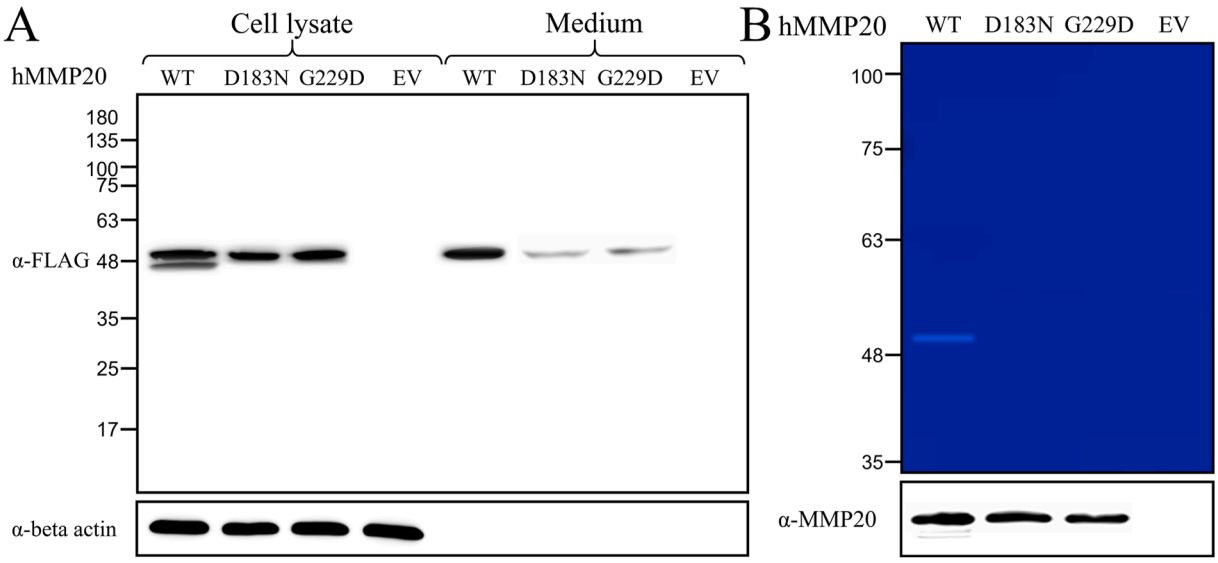

Figure 6 Molecular characterization of human mutant MMP20 proteins. (**A**) Anti-FLAG immunoblotting detected both wild-type and mutant overexpressed human MMP20 proteins in cell lysates and culture media. The signal intensity in the media was weaker for both mutants compared to the wild type. (**B**) Gelatin zymography revealed enzymatic activity only for the wild-type MMP20, despite the expression of both wild-type and mutant proteins. **Key:** hMMP20, human MMP20; WT, wild type; D183N, p.Asp183Asn; G229D, p.Gly229Asp; EV, empty vector.

and among MMP20 paralogs (Fig. 1D). The AlphaMissense prediction gives the p.Gly229Asp mutation a score of 0.9977, indicating its likely pathogenicity. In addition, a *TP63* sequence variant, NG_007550.3:g.302750G>A (NM_003722.5:c.2036G>A), was also identified in the proband. Not found in any databases we scrutinized, this missense variant (NP_003713.3:p.Gly679Glu) is predicted to be "likely pathogenic" with an AlphaMissense pathogenicity score of 0.9322. As *TP63* mutations have been reported to cause enamel hypoplasia,[23] this variant might contribute to proband's enamel defects. Further Sanger sequencing analyses demonstrated that the mother and the sister were heterozygotes for the *MMP20* p.Gly229Asp mutation, while the father carried heterozygous *MMP20* p.Asp183Asn and *TP63* p.Gly679Glu defects.

Family 3

The proband of Family 3 was a 12-year-old boy with generalized enamel defects but was otherwise healthy. No similar malformations were reported among his extended family members (Fig. 3A). Even at the early permanent dentition stage, most of his teeth exhibited rough surfaces with yellowish-brown discoloration due to severe attrition and enamel chipping, particularly on the functional cusps of his posterior teeth (Fig. 3B). In contrast, the mandibular incisors appeared relatively smooth but with apparently thin enamel. Radiographically, the unerupted second molars showed reduced enamel thickness and radiopacity compared to the underlying dentin (Fig. 3C), indicating both hypoplastic and hypomineralized defects.

Exome analysis for the proband identified two heterozygous nonsense mutations in *MMP20*: p.Trp34∗ (c.102G>A) and p.Lys97∗ (g.13436A>T, c.289A>T) (Fig. 3D). The former mutation is identical to one found in Family 1 and a previous case from Taiwan,[21] suggesting a potential founder effect of this mutation on the island. The latter mutation (rs367552668) has never been reported in patients with AI but is documented in gnomAD with a MAF of 0.000045 in the East Asian population. Similar to p.Trp34∗, the p.Lys97∗ variant is expected to result in an *MMP20* null allele, as NMD is likely to be triggered. Further Sanger sequencing confirmed that the father and mother were heterozygous for the p.Trp34∗ and the p.Lys97∗ mutations respectively.

Families 4 and 5

The proband of Family 4 was an adult male who appeared to inherit enamel malformations from the maternal side (Fig. 4A). At the time of recruitment, he had undergone certain dental prosthetic treatments to improve esthetics. The unrestored teeth appeared opaquely white with a mottled yellowish-brown discoloration (Fig. 4B). While the enamel was not particularly thin, dental attrition was evident, especially on first permanent molars, indicating a hypomineralized enamel defect. His mother and one aunt were reported to have similar dental phenotypes to his. The history of fluoride exposure for the family was insignificant.

Family 5 proband was a 2-year-old boy who had enamel hypoplasia and post-eruption failure but was otherwise healthy (Fig. 5A). All his primary teeth exhibited thin enamel, part of which was due to attrition or chipping away of the enamel layer, exposing the underlying dentin (Fig. 5B). Radiographically, the unerupted second primary molars and first permanent molars showed significantly reduced enamel thickness and radiopacity, suggesting hypoplastic and hypomaturation AI. No other family members had noticeable enamel malformations.

Whole exome analyses for all the affected individuals revealed that Family 4 proband and his mother were homozygous for a single-nucleotide duplication in *MMP20* (g.13506dup, c.359dup) (Fig. 4C), while the proband of

Table 1 Human *MMP20* disease-causing mutations.

#	Gene (NG_012151.1)	cDNA (NM_004771.4)	Protein (NP_004762.2)	Ref
1	g.5055_5062dup	c.42_49dup	p.Leu17Serfs*4	11
2	g.5115G>A	c.102G>A	p.Trp34*	Family 1, 3;[21]
3	g.5116A>C	c.103A>C	p.Arg35=	17,24,26
4	g.5145T>G	c.126+6T>G	p.(?)	24,26,27
5	g.13436A>T	c.289A>T	p.Lys97*	Family 3
6	g.13470A>G	c.323A>G	p.Tyr108Cys	24,27
7	g.13506del	c.359del	p.Asn120Ilefs*3	24,28
8	g.13506dup	c.359dup	p.Asn120Lysfs*9	Family 4;[24]
9	g.18444C>T	c.389C>T	p.Thr130Ile	11,17,24,27–29
10	g.20309G>A	c.530G>A	p.Gly177Glu	24
11	g.20318A>G	c.539A>G	p.Tyr180Cys	30
12	g.20319T>A	c.540T>A	p.Tyr180*	29
13	g.20326G>A	c.547G>A	p.Asp183Asn	Family 1, 2
14	g.20345T>C	c.566T>C	p.Leu189Pro	11,24,27
15	g.20390A>G	c.611A>G	p.His204Arg	31
16	g.20395G>A	c.616G>A	p.Asp206Asn	17
17	g.20404G>C	c.625G>C	p.Glu209Gln	10
18	g.21240A>T	c.655A>T	p.Asn219Tyr	32
19	g.21261C>T	c.676C>T	p.His226Tyr	32
20	g.21263T>A	c.678T>A	p.His226Gln	11,16,29
21	g.21271G>A	c.686G>A	p.Gly229Asp	Family 2
22	g.21277C>T	c.692C>T	p.Ala231Val	30
23	g.21295C>A	c.710C>A	p.Ser237Tyr	10
24	g.21393T>C	c.808T>C	p.Tyr270His	11
25	g.21394_21408delinsCCAG	c.809_811+12delinsCCAG	p.(?)	10
26	g.23755G>A	c.910G>A	p.Ala304Thr	11,19,24,27
27	g.23756C>G	c.911C>G	p.Ala304Gly	11
28	g.23778del	c.933del	p.Glu311Aspfs*59	32
29	g.35574A>T	c.954-2A>T	p.(?)	Family 5;[9–11,24,26,27,33]
30	g.35574A>G	c.954-2A>G	p.(?)	11
31	g.35668C>T	c.1046C>T	p.Ala349Val	11
32	g.35676G>A	c.1054G>A	p.Glu352Lys	31
33	g.36769A>C	c.1122A>C	p.Gln374His	10
34	g.36773C>T	c.1126C>T	p.Gln376*	24
35	g.52906G>A	c.1352-1G>A	p.(?)	11
36	g.52917C>G	c.1362C>G	p.Tyr454*	24

Family 5 carried a splice site mutation (g.35574A>T, c.954-2A>T) in both his *MMP20* alleles (Fig. 5C). The c.954-2A>T variant has been shown to cause AI in multiple families with various ethnicities.[11] In contrast, the *MMP20* c.359dup variant had not been reported until it was recently found in a female patient with pigmented hypomaturation AI, who was compound heterozygous for this mutation and the c.954-2A>T defect.[24] The duplication causes a frameshift (p.Asn120Lysfs*9) and introduces a premature stop codon (TAA) in Exon 3, which likely triggers NMD of the mutant transcript and leads to a null *MMP20* allele. Notably, while being rare, this loss-of-function variant (rs759614533) has an allele frequency of 0.00003 globally and among individuals of European descent, according to the gnomAD database. This frequency allows for the possibility of homozygosity, particularly in genetically related communities. Therefore, although consanguinity was not reported in Family 4, the proband, his mother, and aunt were all homozygous for the variant and affected by AI, which gave the appearance of dominant inheritance in the pedigree (Fig. 4A).

Molecular characterization of *MMP20* missense mutations

To assess whether the identified missense mutations, p.Asp183Asn and p.Gly229Asp, impair MMP20 function, we overexpressed the corresponding proteins in HEK293T cells. Immunoblotting revealed reduced levels of both mutant proteins in the culture media compared to the wild type, while intracellular signals from cell lysates remained similar, suggesting impaired secretion of the mutant proteins (Fig. 6A). Gelatin zymography further showed no detectable proteolytic activity for either mutant despite successful expression, indicating a loss of enzymatic function (Fig. 6B). These findings demonstrate that both p.

Asp183Asn and p.Gly229Asp are loss-of-function, disease-causing mutations.

Discussion

To date, 36 different *MMP20* pathogenic variants have been reported (Table 1), including 21 missense, 5 nonsense, 4 frameshift, 5 splice site mutations, and a synonymous variant (c.103A>C) that was shown to decrease Exon 1 definition and cause reduced expression.[17] Among the 21 missense variants, 15 are in the catalytic domain, highlighting the essential proteolytic function of MMP20 during enamel formation. The p.Asp183Asn mutation, identified in this study, alters an aspartic acid residue (Asp^{183}) known to participate in the binding of the second calcium ion within the catalytic domain of all the characterized MMPs.[25] Substitution of this evolutionarily conserved residue is likely to destabilize the domain structure and impair the enzymatic activity of MMP20. Similarly, the other missense mutation reported here, p.Gly229Asp, is located at the active site consensus motif (HEXXHXXGXXH) of the catalytic domain and substitutes an aspartic acid for a small residue, Gly^{229}, right before His^{230}, the second histidine critical for catalytic zinc-binding. Presumably, the mutation will significantly impact the cleavage mechanism at the active site and result in a loss of function. Our immunoblotting and zymographic analyses further validated these predictions, demonstrating that the two *MMP20* missense mutations cause AI by impairing protein secretion and abolishing enzymatic activity.

In summary, this study identified biallelic *MMP20* mutations in five AI families and demonstrated that the affected catalytic domain residues, Asp^{183} and Gly^{229}, are essential for MMP20 function.

Declaration of competing interest

The authors have no conflicts of interest relevant to this article.

Acknowledgments

We thank the individuals and families who participated in this study and the staff at the Biomedical Resource Core, First Core Labs, National Taiwan University College of Medicine, for their technical assistance with molecular cloning and plasmid construction. This study was supported by Ministry of Science and Technology in Taiwan (MOST) grants, 108-2314-B-002-038-MY3 (S.-K. Wang) and 111-2314-B-002-111-MY3 (S.-K. Wang); National Taiwan University Hospital (NTUH) grants, 113-S0006 (S.-K. Wang) and 113-UN0041 (Y.-L. Wang); and National Institutes of Health grants, R01DE027675 (J.P. Simmer) and R56DE015846 (J.C.-C. Hu).

References

1. Hu JC, Chun YH, Al Hazzazzi T, Simmer JP. Enamel formation and amelogenesis imperfecta. *Cells Tissues Organs* 2007;186:78—85.
2. Simmer JP, Richardson AS, Hu YY, Smith CE, Hu JC. A post-classical theory of enamel biomineralization and why we need one. *Int J Oral Sci* 2012;4:129—34.
3. Simmer JP, Hu JC. Expression, structure, and function of enamel proteinases. *Connect Tissue Res* 2002;43:441—9.
4. Lu Y, Papagerakis P, Yamakoshi Y, Hu JC, Bartlett JD, Simmer JP. Functions of KLK4 and MMP-20 in dental enamel formation. *Biol Chem* 2008;389:695—700.
5. Bartlett JD, Simmer JP. Proteinases in developing dental enamel. *Crit Rev Oral Biol Med* 1999;10:425—41.
6. Caterina JJ, Skobe Z, Shi J, et al. Enamelysin (matrix metalloproteinase 20)-deficient mice display an amelogenesis imperfecta phenotype. *J Biol Chem* 2002;277:49598—604.
7. Yamakoshi Y, Richardson AS, Nunez SM, et al. Enamel proteins and proteases in Mmp20 and Klk4 null and double-null mice. *Eur J Oral Sci* 2011;119(Suppl 1):206—16.
8. Hu Y, Smith CE, Richardson AS, Bartlett JD, Hu JC, Simmer JP. Mmp20, Klk4, and Mmp20/Klk4 double null mice define roles for matrix proteases during dental enamel formation. *Mol Genet Genomic Med* 2016;4:178—96.
9. Kim JW, Simmer JP, Hart TC, et al. MMP-20 mutation in autosomal recessive pigmented hypomaturation amelogenesis imperfecta. *J Med Genet* 2005;42:271—5.
10. Nikolopoulos G, Smith CEL, Poulter JA, et al. Spectrum of pathogenic variants and founder effects in amelogenesis imperfecta associated with MMP20. *Hum Mutat* 2021;42:567—76.
11. Wang SK, Zhang H, Chavez MB, et al. Dental malformations associated with biallelic MMP20 mutations. *Mol Genet Genomic Med* 2020;8:e1307.
12. Meredith RW, Gatesy J, Cheng J, Springer MS. Pseudogenization of the tooth gene enamelysin (MMP20) in the common ancestor of extant baleen whales. *Proc Biol Sci* 2011;278:993—1002.
13. Meredith RW, Zhang G, Gilbert MT, Jarvis ED, Springer MS. Evidence for a single loss of mineralized teeth in the common avian ancestor. *Science* 2014;346:1254390.
14. Massova I, Kotra LP, Fridman R, Mobashery S. Matrix metalloproteinases: structures, evolution, and diversification. *FASEB J* 1998;12:1075—95.
15. Arendt Y, Banci L, Bertini I, et al. Catalytic domain of MMP20 (Enamelysin) - the NMR structure of a new matrix metalloproteinase. *FEBS Lett* 2007;581:4723—6.
16. Ozdemir D, Hart PS, Ryu OH, et al. MMP20 active-site mutation in hypomaturation amelogenesis imperfecta. *J Dent Res* 2005;84:1031—5.
17. Kim YJ, Kang J, Seymen F, et al. Alteration of exon definition causes amelogenesis imperfecta. *J Dent Res* 2020;99:410—8.
18. Ryu OH, Fincham AG, Hu CC, et al. Characterization of recombinant pig enamelysin activity and cleavage of recombinant pig and mouse amelogenins. *J Dent Res* 1999;78:743—50.
19. Lee SK, Seymen F, Kang HY, et al. MMP20 hemopexin domain mutation in amelogenesis imperfecta. *J Dent Res* 2010;89:46—50.
20. Karczewski KJ, Francioli LC, Tiao G, et al. The mutational constraint spectrum quantified from variation in 141,456 humans. *Nature* 2020;581:434—43.
21. Papagerakis P, Lin HK, Lee KY, et al. Premature stop codon in MMP20 causing amelogenesis imperfecta. *J Dent Res* 2008;87:56—9.
22. Cheng J, Novati G, Pan J, et al. Accurate proteome-wide missense variant effect prediction with AlphaMissense. *Science* 2023;381:eadg7492.
23. Wright JT, Carrion IA, Morris C. The molecular basis of hereditary enamel defects in humans. *J Dent Res* 2015;94:52—61.
24. Bloch-Zupan A, Rey T, Jimenez-Armijo A, et al. Amelogenesis imperfecta: Next-generation sequencing sheds light on Witkop's classification. *Front Physiol* 2023;14:1130175.
25. Tallant C, Marrero A, Gomis-Rüth FX. Matrix metalloproteinases: fold and function of their catalytic domains. *Biochim Biophys Acta* 2010;1803:20—8.

26. Prasad MK, Geoffroy V, Vicaire S, et al. A targeted next-generation sequencing assay for the molecular diagnosis of genetic disorders with orodental involvement. *J Med Genet* 2016;53:98—110.
27. Gasse B, Prasad M, Delgado S, et al. Evolutionary analysis predicts sensitive positions of MMP20 and validates newly- and previously-identified MMP20 mutations causing amelogenesis imperfecta. *Front Physiol* 2017;8:398.
28. Gasse B, Karayigit E, Mathieu E, et al. Homozygous and compound heterozygous MMP20 mutations in amelogenesis imperfecta. *J Dent Res* 2013;92:598—603.
29. Kim YJ, Kang J, Seymen F, et al. Analyses of MMP20 missense mutations in two families with hypomaturation amelogenesis imperfecta. *Front Physiol* 2017;8:229.
30. Wang SK, Zhang H, Wang YL, et al. Phenotypic variability in LAMA3-associated amelogenesis imperfecta. *Oral Dis* 2023;29:3514—24.
31. Seymen F, Park JC, Lee KE, et al. Novel MMP20 and KLK4 mutations in amelogenesis imperfecta. *J Dent Res* 2015;94:1063—9.
32. Hany U, Watson CM, Liu L, et al. Genetic screening of a non-syndromic amelogenesis imperfecta patient cohort using a custom smMIP reagent for selective enrichment of target loci. *Hum Mutat* 2025;2025:8942542.
33. Wright JT, Torain M, Long K, et al. Amelogenesis imperfecta: genotype-phenotype studies in 71 families. *Cells Tissues Organs* 2011;194:279—83.